ELSEVIER

Flux pinning, surface and geometrical barriers in YNi_2B_2C

S.S. James [a,*], C.D. Dewhurst [b,1], R.A. Doyle [a,2], D.McK. Paul [b], Y. Paltiel [c], E. Zeldov [c], A.M. Campbell [a]

[a] *Interdisciplinary Research Centre in Superconductivity, University of Cambridge, Madingley Road, Cambridge CB3 0HE, UK*
[b] *Department of Physics, University of Warwick, Coventry CV4 7AL, UK*
[c] *Department of Condensed Matter Physics, Weizmann Institute of Science, Rehovot, Israel*

Abstract

In the majority of the $(RE)Ni_2B_2C$ family of superconductors (RE = Dy, Ho, Er, Tm, Y, Lu), a magnetic ordering of the RE moments (RE = Dy, Ho, Er, Tm) appears to directly influence the formation and structure of the vortex lattice as well as the weak residual flux pinning properties. To study the residual pinning in these materials, it is, therefore, necessary to investigate the non-magnetic members such as YNi_2B_2C or $LuNi_2B_2C$, without the influence of magnetic order. Here, we present data from local Hall probe and global magnetization measurements used to examine flux pinning and superconducting hysteresis in YNi_2B_2C ($T_c \approx 15.8$ K). At high fields, a pronounced peak effect in the magnetization indicates that bulk pinning becomes significant as the vortex lattice softens for fields approaching B_{c2}. On the other hand, for small applied fields close to H_{c1}, direct measurements of the local induction using linear micro-Hall probe arrays show dome-like field profiles, as expected when surface and geometrical barrier effects dominate the vortex behaviour over bulk pinning. We discuss the competing roles of weak residual bulk pinning and surface and geometrical barrier effects in YNi_2B_2C. © 2000 Elsevier Science B.V. All rights reserved.

Keywords: Hall probing; RNi_2B_2C; Flux pinning; Surface barrier; Geometrical barrier

The rare-earth nickel borocarbides ([RE]Ni_2B_2C) form an interesting series of materials, which can exhibit both superconductivity and magnetic ordering for members in which RE = Dy, Ho, Er and Tm. Reviews of the magnetic order, superconductivity and crystal structure of the borocarbide materials are given in Refs. [1,2]. Pinning in [RE]Ni_2B_2C is known to be rather weak and the platelet specimens typically grown for measurement are expected to show significant edge barrier effects. Previous measurements do indeed show a strong influence of geometrical effects as well as interactions between the vortex lattice and a particular ordering of the magnetic sublattice [3]. Here, we report local and global magnetization measurements of the non-magnetic YNi_2B_2C to probe the residual pinning properties in the absence of magnetic ordering effects.

YNi_2B_2C crystals were grown by a high-temperature flux method as described elsewhere [4]. Regular shaped crystals were separated from the Ni_2B_2 flux

---

* Corresponding author.
[1] Current address: Institute Laue-Langevin, Grenoble BP156-38042, France.
[2] Current address: Scientific Generics, Harston Mill, Harston, Cambridge CB2 5NH, UK.

and cut into bars with dimensions $\approx 200 \times 90 \times 70$ μm^3 using a miniature wire saw while retaining at least one optically smooth, as-prepared crystal surface ($\perp c$). GaAs/GaAlAs Hall arrays [5] of 11 sensors of active area 10×10 μm^2 and spacing 10 μm were used to make local magnetization measurements. Samples were mounted directly onto the surface (closer than λ) of the array. Larger samples ($\approx 2 \times 2 \times 0.6$ mm^3) were prepared for global magnetization measurements made using an Oxford Instruments vibrating sample magnetometer.

Fig. 1 shows representative local magnetization loops and field profiles for a typical platelet YNi_2B_2C single crystal at 7.54 K. In Fig. 1a, the local magnetization, $B_z - B_s$, has been determined from the measured induction, B_z, by subtraction of the surface field, B_s (sensor 1). Here, we show curves determined by sensors 6 and 4, positioned at the centre and inner edge of the sample, respectively. Hysteresis in the local magnetization is apparent, indicating that flux entry and exit from the sample is subject to either bulk pinning, surface or geometrical barrier effects, which impede flux motion. Inspection of the magnetization curves shows a moderate asymmetry in the hysteretic response with a flat descending field leg, suggesting that bulk pinning is weak and that hysteresis may result from surface [6] or geometrical [5] barrier effects. Here, we make no attempt to distinguish between these two distinct mechanisms, which can result in rather similar magnetic behaviour. Comparison of the two magnetization curves for the sample centre and edge at fields close to and above the full penetration field, H_p, shows that flux penetration and accumulation appear to occur more readily at the sample centre rather than the edge, which consequently exhibits the largest hysteresis. This is confirmed by the increasing field profile shown in Fig. 1b, which shows a large gradient in the local field between the outer (sensor 3) and inner (sensor 4) edge of the crystal and implies that large screening currents flow on the sample edge. For fields greater than H_p, a 'dome-like' field profile is observed with flux accumulation predominantly at the sample centre. This behaviour is in contrast with that expected from bulk pinning and is consistent with the dominance of the geometrical barrier associated with the finite platelet geometry and associated non-uniform demagnetizing field [5,7].
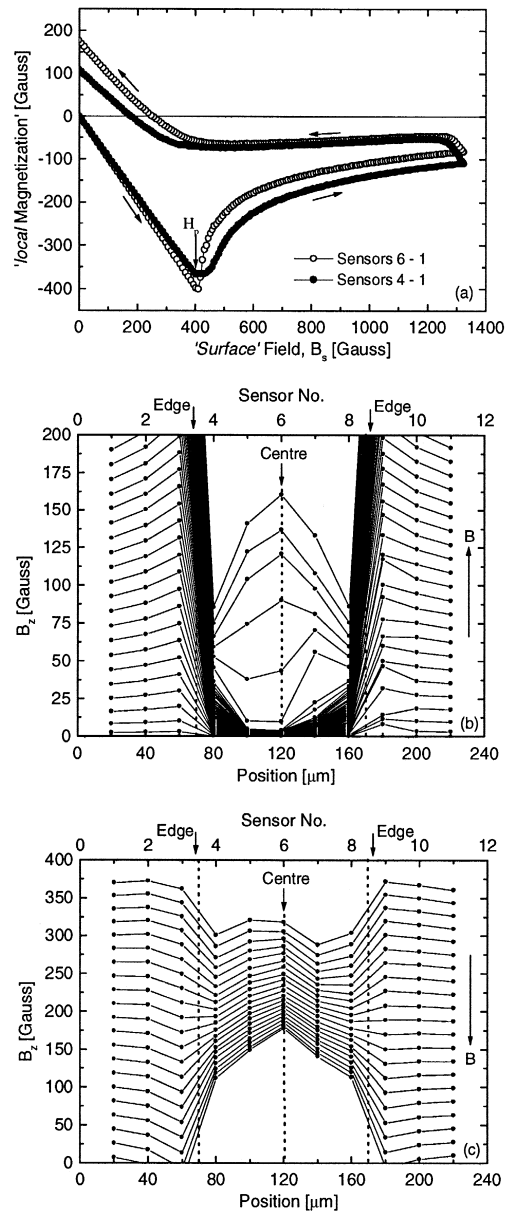

Fig. 1. (a) Local magnetization ($B_z - B_s$) vs. B_s for sensors positioned at the sample centre (6) and edge (4) of a platelet YNi_2B_2C crystal at a temperature of 7.54 K. (b, c) Field profiles measured directly for increasing (b) and decreasing (c) applied field.

Fig. 1c shows the field profiles measured for the decreasing leg of the magnetization curve as the applied field is reduced to zero. For the highest

applied fields, the internal induction is lower than that of the external and applied field due to finite diamagnetism from the reversible surface shielding currents. As the applied field approaches zero, flux exit ceases, resulting in an accumulation of flux again in the sample centre and a finite remanent magnetization (Fig. 1a) as expected for bulk pinning and a residual critical state. This is apparently inconsistent with our observation of dominant surface and geometrical barriers in increasing field, since pinning effects should be symmetric with respect to the field ramp direction and surface or geometrical barriers should not operate significantly for decreasing applied magnetic field. On the other hand, in increasing field, the internal field is zero below H_p, and then very quickly rises as the applied field exceeds H_p. Thus, the effects of bulk pinning at low fields are evident only in a narrow field range above H_p before becoming masked by the geometrical mechanisms. The effects of the weak bulk pinning at low fields are observed more clearly as a remanent flux pool upon decreasing the applied field to zero.

Non-uniformities in the field penetration into the sample are apparent in Fig. 1b. Flux penetrates first to the right of the sample, with the fully established dome only forming afterwards at higher fields. A similar behaviour has been observed by decoration measurements of $NbSe_2$ [8], and more recently by magneto-optical investigations of the similar material $ErNi_2B_2C$ [9]. Zeldov et al. [10] have theoretically

shown that a combination of geometrical barrier effects and bulk pinning lead to the formation of 'double domes' in long strip-shaped samples or flux 'bubbles' for random sample geometries. We believe that the non-uniformities that we observe are such flux 'bubbles', and are, hence, further evidence for a competition between weak bulk pinning and geometrical effects in platelet samples of YNi_2B_2C.

Analysis of the field gradient, dB_z/dx, allows us to differentiate more precisely between surface barriers and bulk pinning [3,5]. Here, we approximate dB_z/dx as the difference between induction measured at the sample centre (sensor 6) and an adjacent probe closer to the sample edge (sensor 5), divided by their separation (20 μm). Fig. 2 shows dB_z/dx calculated in this way as a function of applied field (Fig. 2a) measured over a range of temperatures between 2 and 16 K for a similar YNi_2B_2C crystal. The top panel of Fig. 2a at 7.5 K shows that dB_z/dx is always positive and traces out a clockwise loop, consistent with surface and geometrical barriers dominating the hysteretic response. Positive dB_z/dx in increasing field corresponds to the dome-shaped internal field profile (Fig. 1b) while in decreasing field dB_z/dx is close to zero for fields greater than about 500 G corresponding to the almost flat descending field profile. Below 500 G, dB_z/dx rises rapidly to a positive value corresponding to the trapped vortex 'pool' noted in Fig. 1c. A similar construction is presented in the bottom panel of Fig.
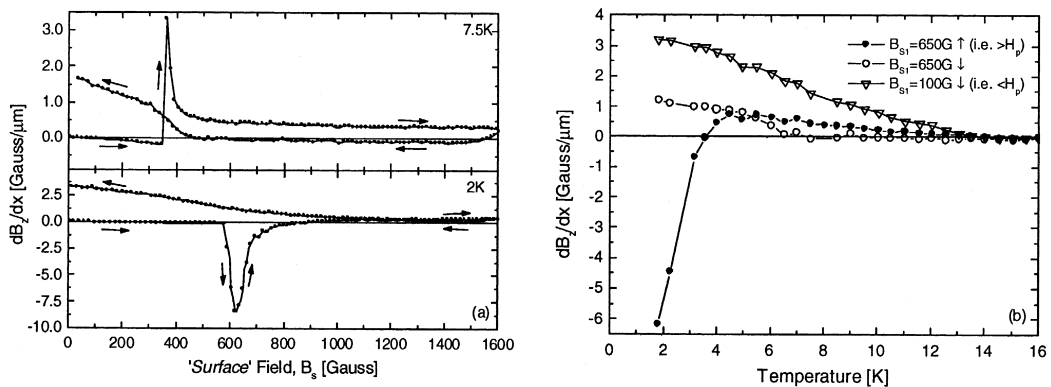

Fig. 2. (a) dB_z/dx vs. B_s for field profiles similar to those shown in Fig. 1(b,c) at 7.5 K (top panel) and 2 K (bottom panel). Clockwise (anticlockwise) direction of the loops is due to surface and geometrical barriers (bulk pinning). (b) dB_z/dx vs. temperature for increasing (solid symbols) and decreasing (open symbols) applied field at 100 G (triangles) and 650 G (circles), lower and greater than H_p, respectively, over this temperature range.

2a for data measured at 2 K. Here, the magnitude of dB_z/dx is now much larger than at 7.5 K and traces an anti-clockwise loop indicating that bulk pinning effects dominate the hysteresis at low temperatures. An estimate for the critical current density can be made directly from the gradient of the field profile in Fig. 2a at 2 K and is of the order of 10^4 A cm^{-2} for fields close to H_p, indicating that bulk pinning is weak when it appears.

Fig. 2b shows dB_z/dx as a function of temperature, at two fixed fields of 100 and 650 G, chosen such that they remain less than or greater than H_p over the measured temperature range, respectively. At 100 G (triangles), dB_z/dx for decreasing field effectively plots the magnitude of the remanent trapped flux pool upon returning to zero field, which increases continuously with decreasing temperature from T_c. On the other hand, for fields greater than H_p (650 G — circles), a positive dB_z/dx in increasing field shows the dominance of surface and geometrical barriers while negative dB_z/dx indicates that bulk pinning dominates the response. For this applied field (650 G), a continuous cross-over between these competing hysteresis mechanisms can be seen between temperatures of about 4 and 6 K. Thus, the low field magnetic hysteresis in platelet crystals of YNi$_2$B$_2$C appears to be determined by a competition between significant surface and geometrical barrier effects and weak residual bulk pinning.

Finally, in Fig. 3, we present high-field global magnetization data for a much larger YNi$_2$B$_2$C single crystal. A larger single crystal not only provides a larger absolute moment for detection, but also changes the relative components of the overall magnetic moment due to either surface (M $\propto d^2$, $d =$ sample dimension $\perp B$) or bulk (M $\propto d^3$) current flow. In Fig. 3, we present the extracted 'critical' current density, J_c vs. applied field, determined using the Bean model and the assumption of bulk pinning and a critical state. Clearly, the Bean model is not valid for low fields close to H_p, where we have shown surface and geometrical barrier effects to be dominant. On the other hand, for fields many times greater than H_p, these barrier effects are expected to be negligible and any remaining hysteresis to be a feature of bulk pinning. Fig. 3 indeed shows the presence of bulk pinning in YNi$_2$B$_2$C at high fields where J_c vs. B shows a pronounced peak
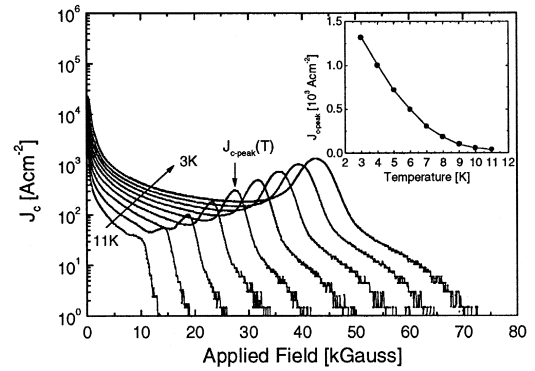

Fig. 3. J_c vs. field determined from the global magnetization curves for temperatures between 3 and 11 K. A pronounced peak-effect at high fields, close to B_{c2}, indicates the existence of residual bulk pinning in YNi$_2$B$_2$C over this temperature range. J_{c-peak} (inset) increases continuously with decreasing temperature.

effect for fields close to B_{c2}. Data are presented for temperatures between 3 and 11 K, confirming the existence of residual bulk pinning in YNi$_2$B$_2$C over this temperature range. At 3 K, an estimate for J_c is of the order 10^3 A cm^{-2}; an order of magnitude less than that determined locally at low applied fields, but consistent with an anticipated field dependent J_c. The inset to Fig. 3 shows J_{c-peak} vs. temperature.

In conclusion, we find an interplay between weak bulk pinning and surface and geometrical barrier effects at low fields close to H_p. Surface and geometrical barriers dominate the magnetic behaviour above about 4 K, resulting in dome-like internal field profiles and asymmetric hysteresis at low fields. Asymmetry in the field profiles has been resolved and is thought to be consistent with magneto-optical and decoration observations of 'bubble-like' flux penetration in other weak pinning superconductors. Below 4 K, bulk pinning becomes strong enough to be visible in increasing field profiles as a critical state at low fields. Global magnetization measurements show a peak effect in the magnetic moment for fields close to B_{c2}, confirming the existence of weak residual pinning over a wide temperature range below T_c. Magnetic hysteresis in YNi$_2$B$_2$C for fields close to H_p is determined by an interplay between weak bulk pinning and significant edge barrier effects, which should not be overlooked in the analysis of low field vortex properties.

References

[1] J.W. Lynn, S. Skanthakumar, Q. Huang, S.K. Sinha, Z. Hossain, L.C. Gupta, R. Magarajan, C. Godart, Phys. Rev. B 55 (1997) 6584.

[2] P.C. Canfield, P.L. Gammel, D.J. Bishop, Phys. Today 51 (1998) 40.

[3] C.D. Dewhurst, R.A. Doyle, E. Zeldov, D.McK. Paul, Phys. Rev. Lett. 82 (1999) 827.

[4] M. Xu, P.C. Canfield, J.E. Ostenson, D.K. Finnemore, B.K. Cho, Z.R. Wang, D.C. Johnston, Physica C 227 (1994) 321.

[5] E. Zeldov, D. Majer, M. Konczykowski, A.I. Larkin, V.M. Vinokur, V.B. Geshkenbein, N. Chikumoto, H. Shtrikman, Europhys. Lett. 30 (1995) 367.

[6] C.P. Bean, J.D. Livingston, Phys. Rev. Lett. 12 (1964) 14.

[7] E.H. Brandt, Phys. Rev. B 59 (1999) 3369.

[8] M. Marchevsky, L.A. Gurevich, P.H. Kes, J. Aarts, Phys. Rev. Lett. 75 (1995) 2400.

[9] N. Saha, P.H., Kes, 1999, unpublished.

[10] E. Zeldov, A.I. Larkin, V.B. Geshkenbein, M. Konczykowski, D. Majer, B. Khaykovich, V.M. Vinokur, H. Shtrikman, Phys. Rev. Lett. 73 (1994) 1428.